https://ntrs.nasa.gov/search.jsp?R=19690010323 2020-03-12T07:37:45+00:00Z

N69-19677
CR-100316

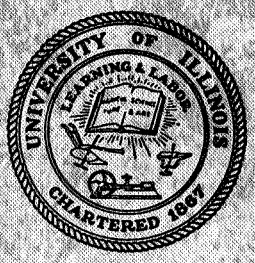

T.&A.M. REPORT NO. 319

ENHANCED GRAIN BOUNDARY SLIDING DURING REVERSED CREEP OF LEAD

by

Masaki Kitagawa

Sponsored by

National Aeronautics and Space Administration
Lewis Research Center
Research Grant NGR 14-005-025

DEPARTMENT OF THEORETICAL AND APPLIED MECHANICS
UNIVERSITY OF ILLINOIS
URBANA, ILLINOIS

T. & A. M. DEPARTMENT REPORTS:

The Department of Theoretical and Applied Mechanics at the University of Illinois, established in 1890 as a separate unit of the College of Engineering, has the following threefold purpose: (1) to offer instruction in engineering mechanics to undergraduate students, (2) to teach and train graduate students in the field of mechanics, and (3) to conduct a comprehensive research program resulting in the extension of knowledge in all branches of mechanics and related fields. From its inception, the department has offered courses in mechanics in partial fulfillment of the degree requirements of the other departments of the College and, since 1957, the degree of *Bachelor of Science* in Engineering Mechanics has been administered by the department. The granting of graduate degrees originated in 1908, both *Master of Science* and *Doctor of Philosophy* degrees being offered. Research is considered to be a basic part of the educational program; strong emphasis is placed on the fact that the functions of teaching and research go hand in hand for the most complete and effective development of both students and staff.

In general, the research studies are of a fundamental nature that supplement the regular educational functions of the department. They either show the application of the accepted concepts of the engineering sciences to problems in widely divergent fields or produce new concepts with which to attack specialized aspects of problems. Current projects are in the fields of mechanical properties of materials, mechanics of fluids, mechanics of solids, and dynamics. Many of these studies are of a complex analytical nature. However, extensive facilities and unique special equipment are also available for research and advanced study of engineering components which operate under extreme environmental conditions that lead to new problems for which standard design procedures are inadequate. Ten different laboratories are operated with special facilities for studies of concrete, fluid mechanics, fatigue, properties of metals, plastics, vibration, photoelasticity, creep, railroad rails and wheels, and experimental strain measurements employing electronic instrumentation.

The results of research studies conducted in the department are generally disseminated in *T. & A. M. Department Reports*. These present information of an enduring nature, such as the final report of a research contract, and in turn are given a wide initial distribution. After the remainder of the initial printing has been requested and distributed, copies are available on loan (or on purchase in microfilm form)* from the Acquisitions Department of the Library, University of Illinois, Urbana, Illinois. A list of recent reports is included inside the back cover of this report.

For further information address inquiries to:

T. J. Dolan, Head of the Department
212 Talbot Laboratory
Urbana, Illinois

* Charges for microfilm copy are 4¢ per exposure plus mailing cost and 25¢ service charge.

T. & A. M. Report No. 319

ENHANCED GRAIN BOUNDARY SLIDING DURING REVERSED CREEP OF LEAD

by

Masaki Kitagawa

Sponsored by

National Aeronautics and Space Administration
Lewis Research Center
Research Grant NGR 14-005-025

Department of Theoretical and Applied Mechanics
University of Illinois, Urbana

October 1968

ABSTRACT

Chemical lead is subjected to multiple creep stress reversals at room temperature, 100 C and 150 C, and the alterations in grain structure are examined.

Creep deformation resistance at these test temperatures decreases significantly under multiple stress reversals. However, the decrease in creep resistance caused by reversed stressing is smaller when the test temperature is increased above about half of the melting point of the metal.

Significant microstructural changes are observed during reversed creep. Grain boundaries are found to migrate toward planes of maximum shear stress, resulting in an orthorhombic grain structure.

The formation of this unusual grain structure is discussed in relation to creep resistance changes due to reversed stressing. To support the discussion, grain boundary sliding during reversed creep was measured. The contribution of grain boundary sliding to the total creep strain is found to greatly increase as the orthorhombic grain structure is formed.

ACKNOWLEDGMENT

This work was conducted in the H. F. Moore Fracture Research Laboratory of the Department of Theoretical and Applied Mechanics at the University of Illinois. Financial support was provided by the National Aeronautics and Space Administration under Research Grant NGR 14-005-025.

The author is deeply indebted to Professor JoDean Morrow and Professor T. J. Dolan, Head of the Department for their continued encouragement and support. I also wish to thank Professor S. Taira, Kyoto University, Japan, who introduced me to this field of research and arranged for me to study in the United States.

TABLE OF CONTENTS

1. INTRODUCTION

The creep deformation resistance of metals may change significantly due to repeated reversals of the creep stress. In the case of chemical lead at room temperature, Morrow and Halford (1) have reported that after about 60 stress reversals the static creep rate increases approximately ten times compared to the virgin creep rate.

From the limited amount of work in the literature which is summarized in Table 1 (1-7), the nature of reversed creep may be briefly stated as follows:

1. At low homologous temperatures, the creep resistance increases with number of stress reversals (2, 3).
2. At high homologous temperatures, however, the creep resistance significantly decreases due to reversed stressing (1, 2, 4).
3. This decrease in creep resistance at high homologous temperatures is persistent in nature causing a permanent alteration in creep deformation resistance (5).
4. Acceleration of creep due to stress reversals has been observed for several modes of deformation and for a variety of metals provided the test temperature is high enough.

Above a test temperature of about 0.4 T_m*, a decrease in creep resistance during reversed creep may be expected (Fig. 1). Significant changes in the microstructure of the metal may accompany the decrease in creep resistance at high temperatures. However, no extensive study has yet been made of the influence of reversed creep on the structure of metals.

The purpose of this paper is to examine in detail the microstructure of specimens subjected to reversed creep and to relate the observations to creep resistance alteration.

---

* T_m is the absolute melting temperature of a particular metal.

2. EXPERIMENTS

2.1 Material and Specimen

Tubular specimens were machined from 1-1/4 in diameter rods of chemical lead. The chemical composition and specimen geometry are shown in Table 2 and Fig. 2.

After machining, the outer surface of the reduced section was chemically polished by means of a mixture of two parts of H_2O_2 (30% purity) and eight parts of glacial acetic acid in an ice bath. Because of the low melting point of lead, mechanical polishing or sectioning at room temperature tends to recrystallize the surface metal. For this reason, cut surfaces were carefully removed to a depth of at least one millimeter by means of chemical polishing.

2.2 Creep Testing Apparatus and Test Method

A hydraulic torsional creep testing machine was used which employs closed loop control (8). Zero clamping force and concentricity of rotational motion were obtained by the use of a split tapered collet on one end of the specimen and a splined shaft fastened to the torque frame through a Wood's metal pot on the other end (2).

Shear strain was calculated from the angle of twist measured between shoulders of specimen by an R. V. D. T. (rotary variable differential transformer). A gage length of 1.4 in was used for the calculation of shear strain. Average creep rate, $\bar{\gamma}$, as defined in Fig. 3, was calculated by dividing the creep strain by the period of one reversal.

Internal resistance heating was used for tests at 100 C and 150 C. The heating element is a 1/4 in diameter stainless steel rod with two reduced sections of 3/16 in diameter and 1-1/4 in length. It was located at the center of the tubular specimen and powered by a 30 kvA welding transformer.

Temperature was measured on the surface by means of chromel-alumel thermocouples. With this method of heating, the temperature along the gage length varied less than $\pm$ 4 C at test temperatures of 100 C and 150 C.

The test conditions are illustrated in Fig. 3. In each test, the shear stress, τ, was maintained constant until a preset strain limit was reached and then reversed. When the total strain reached zero, the stress was reversed again and maintained constant until the strain limit was reached. Reversing was continued for about 60 to 70 reversals.

2.3 Metallographic Study

The specimen surface, longitudinal, and transverse cross sections were examined under an optical microscope. X-ray back-diffraction patterns were taken on the specimens using Cu-K_α radiation. Average grain size was calculated by making several measurements of the number of grains in an area of 0.4 mm^2.

For periodic examination of the grain structure, replicas were taken from the specimen surface during reversed creep using replicating tape and acetone. Creep stress during this test was $\pm$ 680 psi except during the first and the 71st reversals when the creep stress was $\pm$ 600 psi. This test was frequently interrupted just before the creep stress was reversed and during single creep curves in order to take replicas.

2.4 Calculation of Grain Boundary Sliding Strain

Artificial scratches were inscribed on the specimen surface using either dry cotton or a thin razor blade. Replicas were taken from the scratched surface to measure the amounts of grain boundary sliding, Δu_1 and Δu_2, and the grain length, Δx_1 and Δx_2, under an optical microscope. The directions of Δx_1 and Δx_2 and the positive directions of Δu_1 and Δu_2 are indicated in Fig. 4a. The coordinates, 1 and 2, are directions of maximum shear. The grain boundary sliding strain, γ_{gb}, was calculated by the following equations:

$$\gamma_{gb} = \frac{\Delta u_1}{\Delta x_2} + \frac{\Delta u_2}{\Delta x_1}$$

for the orthorhombic grain structure, and

$$\gamma_{gb} = K \frac{\Delta u_2}{\Delta x_1}$$

for the irregularly shaped grain structure. Where $K = 2$ was used to account for the randomness of boundary orientation. For each calculation of boundary sliding strain more than 20 grain boundaries were examined.

3. EXPERIMENTAL RESULTS

3.1 Creep Test Results

Five specimens of chemical lead were tested at room temperature (0.5 T_m), 100 C (0.62 T_m), and 150 C (0.70 T_m). The test conditions and results are summarized in Table 3 and plotted in Fig. 5. Average creep rates which are plotted in Fig. 5 are the average of two reversals, i.e., of one cycle. Because of frequent interruptions of testing, the average creep rate of Spec. 5 is not plotted in Fig. 5.

For all tests, the average creep rate rapidly increases at first with the number of stress reversals. For tests at room temperature and 100 C, the creep rate continues to increase after the initial rapid change although the rate of increase decreases. At 150 C, however, the average creep rate increases for several cycles and then decreases slightly for several cycles and then increases again. This cyclic nature of creep rate change seems to continue throughout the test.

The average creep rate on the 31st cycle, $\overline{\gamma}_r$, was arbitrarily chosen as representative of the creep rate after reversed stressing for comparison with the average creep rate of virgin specimens, $\overline{\gamma}_o$. Ratios for these two creep rates are listed in Table 3 and plotted in Fig. 1 along with other published data (1-4). A ratio smaller than one indicates an increase in creep resistance during reversed creep and a ratio larger than one indicates a decrease in creep resistance.

Under all test conditions reported in this paper, creep resistance significantly decreases due to stress reversals. However, the degree of decrease in creep resistance, $\overline{\gamma}_r / \overline{\gamma}_o$ is smaller the higher the test temperature, implying that there exists an optimum temperature for the maximum acceleration of creep.

3.2 Results of Metallographic Study

Grain structures before and after reversed creep are shown in Figs. 6a-6d for three test temperatures. Maximum shear directions are vertical and horizontal in the photographs.

The grain structure before testing is of the type ordinarily found, being of irregular shape with randomly oriented boundaries.

During reversed creep at room temperature and 100 C, grain boundaries were found to migrate into a rectangular network. Traces of grain boundary migration are shown in Fig. 7 and the resultant networks in Figs. 6b and 6c. At 150 C, however, recrystallization and grain growth takes place. Figure 6d shows a portion of a recrystallized grain. Grain growth is evident and the grain boundaries are randomly oriented. Consequently, such irregularly shaped grains predominate along the gage length, although some rectangular grain boundaries may still be seen.

Cross sectional views of this grain structure are shown in Figs. 4b and 4d. On both cross sections as well as the circumferential surface, the grain boundaries form into rectangular networks, showing the grain shape to be orthorhombic. In both longitudinal and transverse cross sections, grains are generally longer in one direction. The elongation is in the direction of the intersections of maximum shear planes on these cross sections.

Average grain sizes are also listed in Table 3. Before testing, the average grain size was 0.060 mm. After reversed creep, grain sizes are consistently larger than before. Furthermore, the higher the test temperature, the larger the grain size.

Figures 7a and 7b show the surface of a crept specimen before polishing. Besides the trace of grain boundary migration, slip bands and severely deformed regions are seen. Intense slip bands or severely deformed regions were usually observed near L and T type intersections of new grain boundaries as seen in Fig. 7a, showing that localized intragranular deformation has occurred due to the intergranular sliding.

The observed slip bands at high homologous temperatures are nearly parallel to the maximum shear directions. X-ray diffraction patterns, represented by Fig. 8, did not show any obvious preferred orientation. Therefore, the highly oriented slip bands are not believed to be caused by preferred orientation but rather by the possibility of slip on crystalline planes other than the ordinary {111} , such as {100} , as suggested in Ref. 9.

3.3 Periodic Observations of Grain Structure during Reversed Creep by Means of Replication

A region of the specimen surface was followed during testing by means of replication. The average creep rates, $\overline{\gamma}$, of this test are listed in Table 3.

Figure 9a is the grain structure of a virgin specimen. The three black squares are indentation marks for identification purposes.

During static creep, sharp Y type grain boundary intersections tend to round off, as is seen in grains R and Q of Figs. 9a and 9b. It is also observed that some grain boundaries (for example, grain K) migrate toward the maximum shear directions during static creep. The rectangular grain boundary network is roughly formed during the first few cycles (Fig. 9c). During this time the average creep rate increases rapidly (Fig. 5). After initial formation, the rectangular network is further subdivided. This subdivision development is slow. For example, grain P (Figs. 9d-9f) is subdivided by the gradual boundary migration of a small grain, which took about 40 reversals.

3.4 Grain Boundary Sliding

Grain boundary sliding measurements for the orthorhombic grain structure, were taken in two selected areas for each Δu_1 and Δu_2, so that they represent the regions of well developed rectangular network and of poorly developed rectangular network. In the region of better developed rectangular grain boundaries the grain length is smaller. For calculating γ_{gb}, the average values of $\Delta u_1/\Delta x_2$ and $\Delta u_2/\Delta x_1$ measured in each area were used.

Figure 10 shows an example of measured sliding. It was observed that some grain boundaries require time before sliding begins resulting in a cyclic nature of sliding which has been often observed in boundary sliding measurements (10). Although each boundary slides in a different manner, the average value of $\Delta u_1/\Delta x_2$ or $\Delta u_2/\Delta x_1$ along the length of about 0.6 mm changes smoothly (Table 4).

Figures 11a and 11b compare the total creep strain with the grain boundary sliding strain after the formation of the orthorhombic grain structure. Creep curves of grain boundary sliding are similar to the total creep curves. The ratios, γ_{gb}/γ_t, are 0.65 for $\tau = \pm 680$ psi and 0.80 for $\tau = 600$ psi at $0.5\ T_m$.

For the irregularly shaped grain structure, the obtained values are $\gamma_{gb} = 0.014$ and $\gamma_{gb}/\gamma_t = 0.29$ under $\tau = 600$ psi. These values are less than half of the value obtained after the formation of the orthorhombic grain structure.

4. DISCUSSION

The formation of a rectangular network of grain boundaries on the surface has been reported in the case of high temperature fatigue of lead (11, 12) and aluminum and aluminum alloys (12, 13). The surface structure observed in Refs. (11-13) is similar to the two dimensional view of the orthorhombic structure found in this study of lead subjected to reversed creep.

In the following sections, the significance of the orthorhombic grain structure in reversed creep is discussed.

4.1 Enhancement of Grain Boundary Sliding due to the Formation of Orthorhombic Grain Structure

At high homologous temperatures, grain boundary sliding is more active than at low homologous temperatures. However, because of the irregularity of the grain boundary network in the usual grain structure, sufficient intragranular deformation is required to accommodate grain boundary sliding. Consequently, the intragranular deformation resistance must be the main factor in determining the total creep resistance in the irregularly shaped grain structure, unless there is a drastic change in grain structure.

Formation of the orthorhombic grain structure makes grain boundary sliding easier for two reasons. First, stress on the boundaries is everywhere maximum in the orthorhombic structure. Second, the constraining forces between adjacent grains are probably smaller than in the case of irregularly shaped grains.

This reasoning can be justified by Fig. 12 which was taken after static creep at a shear strain of 0.047. The lines running across the photograph are artificial scratches which were inscribed before the test. Grain boundaries which are not parallel to the maximum shear directions show little boundary sliding. When the boundaries are long and parallel to the maximum shear directions, sliding can be significant. An example is seen in the figure along a vertical boundary $\overline{BC}$. When grain boundaries are parallel to the maximum shear directions but short, sliding is restricted by the adjacent grains near triple points of boundaries. Examples are also

seen in the figure on the boundaries labeled with T's. Grain boundaries in the orthorhombic structure are more like $\overline{BC}$, being long and parallel to the directions of maximum shear.

The measurement of grain boundary sliding gives further numerical support for the above reasoning. Grain boundary sliding contributes more than 50% to the total creep strain after the orthorhombic grain structure has formed for the stress levels investigated. This large contribution was not found for the usual irregularly shaped grain structure.

Figure 13 shows a relationship between $\Delta u_1/\Delta x_2$, $\Delta u_2/\Delta x_1$, and the average grain length in the orthorhombic structure. It is seen that the better developed is the orthorhombic structure (smaller grain length), the larger is the strain due to grain boundary sliding. It would be expected, therefore, that the value of γ_{gb}/γ_t would be even larger than 0.8 for the same test conditions if the subdivision of the rectangular network is further developed by additional stress reversals.

The above discussion shows that, with progressive formation of the orthorhombic grain structure, the resistance to grain boundary sliding becomes more and more the determining factor governing total creep resistance. Constraining forces between adjacent grains are reduced. Also, the total area of the boundaries which lie on the maximum shear planes increases.

4.2 Relation between Changes in Creep Rate and Grain Structure

At this stage of discussion, it is interesting to qualitatively correlate the alteration of creep resistance due to multiple stress reversals and the formation of the orthorhombic grain structure.

During the early stages of a high temperature reversed creep test, there is a rapid increase in average creep rate accompanied by a rapid formation of a rectangular network of grain boundaries. As reversed stressing is continued, there is less increase in the average creep rate and only minor further development of the rectangular network.

As is seen in Fig. 1, the ratio, $\bar{\gamma}_r/\bar{\gamma}_o$, decreases when the test temperature is increased above about half of the melting point of the metal. This is believed to be due to an increase in the size of the orthorhombic grains with increasing temperature until a recrystallized structure predominates. Furthermore, the cyclic nature of creep rate change with the number of stress reversals observed at 150 C may be due to the periodic occurrence of recrystallization which tends to eliminate the orthorhombic grain structure.

At low homologous temperatures, where deceleration of creep has been reported (2,3), the orthorhombic structure may not be formed since the grain boundary migration is unlikely at low homologous temperatures.

The observed orthorhombic grain structure is believed to be quite stable. It was in fact observed that the general view of the rectangular boundary network had not changed at room temperature even two months after testing. Thus, the persistent decrease in creep resistance due to reversed stressing reported in Ref. (5) should be expected.

5. SUMMARY

Torsional reversed creep tests of chemical lead specimens were performed at temperatures of 0.5, 0.62 and 0.70 T_m. The grain structure and the role of grain boundary sliding were examined. The following results were obtained.

1. The creep of chemical lead at these temperatures is significantly accelerated under multiple stress reversals. The degree of the increase in creep rate with the number of stress reversals decreases with an increase in test temperature above about half of the melting point of the metal. This and published results imply that there exists an optimum temperature for maximum acceleration of creep.

2. Grain shape and grain size change significantly during reversed creep. Boundaries migrate to form an orthorhombic grain structure with sides parallel or perpendicular to the maximum shear planes.

3. At a temperature of 0.5 T_m, the contribution of grain boundary sliding to the total creep strain is large after the formation of the orthorhombic grain structure. In the usual irregularly shaped grain structure, however, grain boundary sliding is only a minor part of the total creep strain at the stress levels examined.

4. The formation of the orthorhombic grain structure is believed to be the cause of the acceleration of creep due to stress reversal at high homologous temperatures. Enhanced grain boundary sliding resulting from the orthorhombic structure accounts for the nature of reversed creep observed in this work as well as in earlier research.

LIST OF REFERENCES

1. JoDean Morrow and G. R. Halford, "Creep Under Repeated Stress Reversals," Joint International Conference on Creep: The Institute of Mechanical Engineers, London, 1963, pp. 3-43 to 3-47.

2. C. E. Jaske, "The Influence of Temperature on Reversed Creep," MS Thesis, Department of Theoretical and Applied Mechanics, University of Illinois, 1967. See also T&AM Report No. 674.

3. H. Conrad, "Effect of Changes in Slip Direction on the Creep of Magnesium Crystals," Transactions of the Metallurgical Society of AIME, Vol. 215, Feb. 1959, pp. -63.

4. A. N. Hughes, "Creep of a 20% Cr/25% Ni/Nb Steel Under Reversed Creep Conditions," TRG Report 1018(6), United Kingdom Atomic Energy Authority, 1965.

5. L. B. Freund, Effect of Repeated Stress Reversals on the Creep of Lead," Fourth Student Symposium on Engineering Mechanics, T&AM Report No. 262, Department of Theoretical and Applied Mechanics, University of Illinois, 1964.

6. E. N. da C. Andrade and K. H. Jolliffe, "The Flow of Polycrystalline Metals Under Simple Shears," Proceedings of the Royal Society of London, Vol. 213A, 1952, pp. 3-26.

7. P. W. Davis and B. Wilshire, "Void Growth During Secondary Creep," Philosophical Magazine, Vol. 11, Jan. 1965, pp. 189-190.

8. P. A. Lilienthal, "Description of a Torsion System with Exploratory Data on Accelerated Creep Due to Multiple Stress Reversals," MS Thesis: Department of Theoretical and Applied Mechanics, University of Illinois, 1967.

9. C. S. Barrett, Structure of Metals, McGraw-Hill Book Company, Inc., New York, 1953, p. 337.

10. F. Garofalo, Fundamentals of Creep and Creep Rupture in Metals, The MacMillan Company, New York, 1963, pp. 127-146.

11. K. U. Snowden, "The Effect of Atmosphere on the Fatigue of Lead," Acta Metallurgica, Vol. 12, 1964, pp. 295-303.

12. S. Takeuchi and T. Homma, "On the Characteristics of Grain Boundary Migration in Pure Metals under the Fatigue at Elevated Temperatures," Transactions of the Japan Institute of Metals, Vol. 7, 1966, pp. 39-46.

13. J. T. Blucher and N. J. Grant, "Low Strain Rate, High Strain Fatigue of Aluminum as a Function of Temperature," Transactions of the Metallurgical Society of AIME, Vol. 239, 1967, pp. 805-813.

Table 1 Summary of Published Work on Reversed Creep

Metal & Ref.	Temp.	No. of Stress Reversals	Type & No. of Tests		Remarks
Chemical Pb (1)	0.5 T_m	100	Torsion of tube	13	Acceleration-Creep rate of about ten times as much as creep rate of virgin specimens was observed after 60-100 stress reversals
1100-F Al (2)	0.32-0.55 T_m	60	Torsion of tube	15	Acceleration at high temperature Deceleration at low temperature
Magnesium (3)	0.32 T_m	10	Shear, const. period of 10 mins per rev.	1	Deceleration
20% Cr/25% Ni/ Nb steel (4)	0.55 T_m	83	Axial, const. period of 10 hrs per rev.	1	Acceleration-After each compressive creep test, strain was brought back to zero by tensile force
20% Cr/25% Ni/ Nb steel (4)	0.55 T_m	63	"	1	Acceleration-Both tensile and compressive creep curves were examined
Chemical Pb (5)	0.5 T_m	20	Torsion of tube	8	Acceleration-The steady state creep rate after stress reversals was much larger than that of virgin lead
Commercial Cd (6)	0.5 T_m	1 or 2	Shear of disk	5	Deceleration
Commercial Pb (6)	0.5 T_m	1 or 2	"	5	Acceleration

Table 1 continued

Metal & Ref.	Temp.	No. of Stress Reversals	Type & No. of Tests		Remarks
Spectroscopically Pure Pb (6)	0.5 T_m	1 or 2	Shear of disk	7	Acceleration
Ni-Pd 0.1 at% (7)	0.47 T_m	2	Axial	1	Deceleration-Stress was reversed at tertiary creep stage
Cu/5% Al alloy (7)	0.52 T_m	2	"	1	Deceleration-Stress was reversed at tertiary creep stage

Table 2 Chemical Composition of Chemical Lead

Ag	0.002% <	< 0.020%
Cu	0.040% <	< 0.080%
As + Sb + Sn		< 0.02 %
Zn		< 0.001%
Fe		< 0.002%
Bi		< 0.005%
Pb		> 99.90%
		(ASTM B29-55)

Table 3 Summary of Reversed Creep Data at Temperatures Above 0.5 T_m

Specimen No.	T/T_m	Shear strain range, $\Delta\gamma$	Shear stress amplitude τ_a, psi	Ratio of ave. creep rate,* $\bar{\dot{\gamma}}_r / \bar{\dot{\gamma}}_o$	Ave. grain size after test, mm**
1	0.5	0.047	$\pm$ 640	6.2	0.092
2	0.62	0.050	$\pm$ 460	4.4	0.13
3	0.70	0.030	$\pm$ 280	3.4	1
4	0.70	0.050	$\pm$ 280	2.3	
5***	0.5	0.05	+ 600 (first reversal, $\bar{\gamma} \cong 0.00027$)		
			$\pm$ 680 (2nd-70th reversals, $\bar{\gamma} \cong 0.0011$-$0.0058$)		
			+ 600 (71st reversals, $\bar{\gamma} \cong 0.0026$)		

Note: * The average creep rate on the 31st cycle, $\bar{\dot{\gamma}}_r$, was arbitrarily chosen as representative of the creep rate after reversed stressing, and compared with the average creep rate of virgin specimens, $\bar{\dot{\gamma}}_o$.

** Before the tests, average grain size was 0.060 mm.

*** In order to take replicas, the test was frequently interrupted. Two days rest period at $T = 0.5\ T_m$ was inserted before the 71st reversed creep.

Table 4 Summary of Measurements of Grain Boundary Sliding in Orthorhombic Grain Structure

No. of stress reversals	Macroscopic plastic strain, γ_t	Creep stress, τ	Creep time min.	$\Delta u_2/\Delta x_1$*		$\Delta u_1/\Delta x_2$*		γ_{gb}
				a	b	a	b	
66	0.000	-	0.0	0.0000	0.0000	0.0000	0.0000	0.000
	0.007	+ 680 psi	0.2	0.0039	0.0008	0.0005	0.0003	0.003
	0.017	"	1.4	0.0124	0.0037	0.0012	0.0015	0.009
	0.027	"	2.8	0.0184	0.0073	0.0030	0.0027	0.015
	0.037	"	4.5	0.0248	0.0119	0.0051	0.0034	0.023
	0.0465	"	6.5	0.0287	0.0178	0.0077	0.0042	0.030
67	0.039	- 680 psi	6.7	0.0245	0.0141	0.0068	0.0032	0.024
	0.029	"	8.0	0.0184	0.0091	0.0043	0.0029	0.018
	0.019	"	9.5	0.0117	0.0054	0.0030	0.0027	0.012
	0.009	"	11.5	0.0053	0.0027	0.0019	0.0014	0.006
	0.000	"	13.4	-0.0021	-0.0006	0.0009	0.0001	-0.001
	Two days rest period under no load							
70	0.000	-	0.0	0.0000	0.0000	0.0000	0.0000	0.000
	0.007	+ 600 psi	0.7	0.0060	0.0035	0.0015	0.0013	0.006
	0.017	"	3.6	0.0135	0.0066	0.0030	0.0018	0.013
	0.027	"	7.3	0.0191	0.0109	0.0046	0.0026	0.019
	0.037	"	11.7	0.0255	0.0163	0.0067	0.0035	0.026
	0.0465	"	16.7	0.0365	0.0225	0.0093	0.0050	0.037
Average Grain Length, μ				53	97	132	148	

* Columns a represent the measurements in the region of well developed rectangular network of grain boundaries, and columns b represent those in the region of poorly developed network.

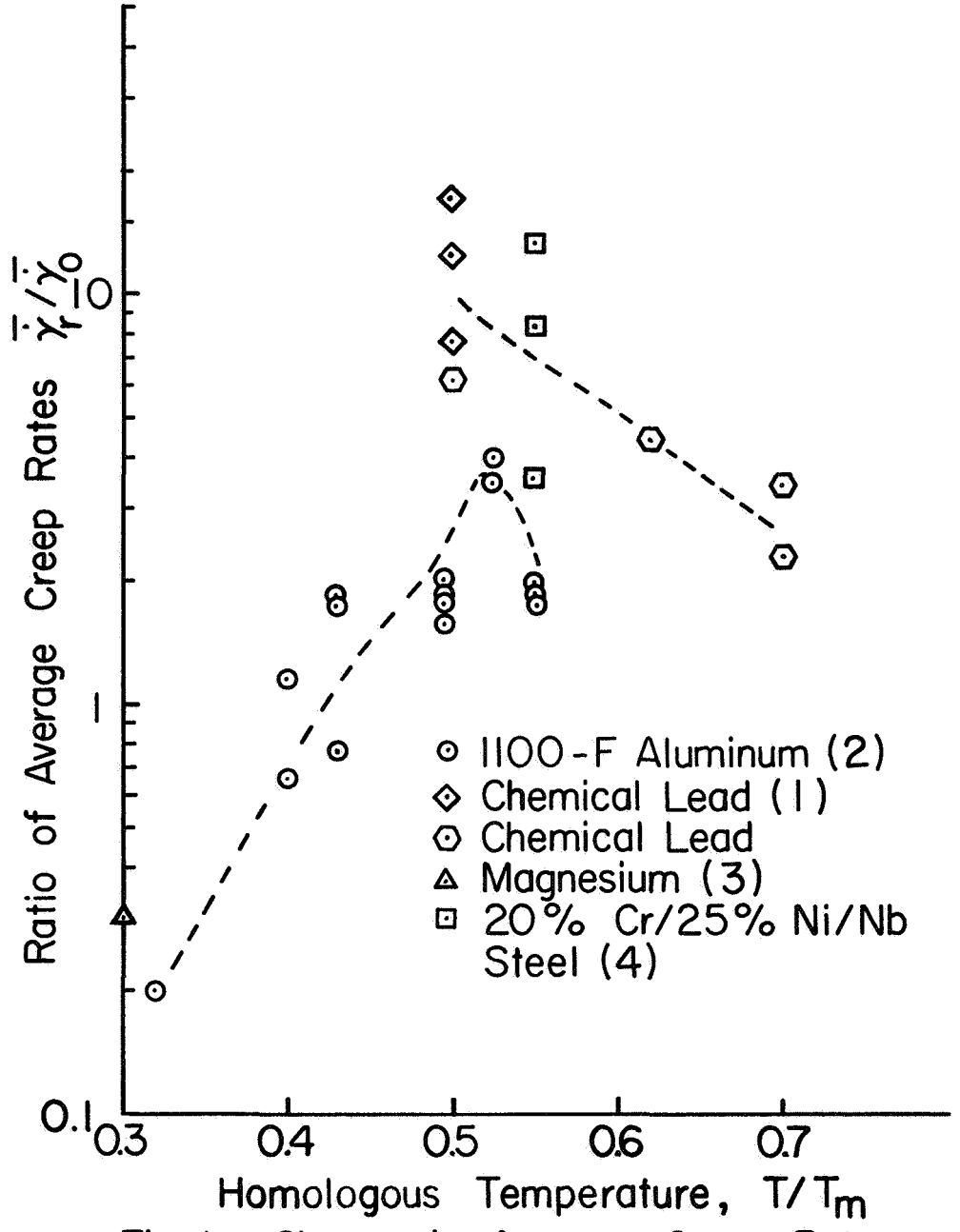

Fig. 1 Change in Average Creep Rate after Multiple Stress Reversals as a Function of Temperature

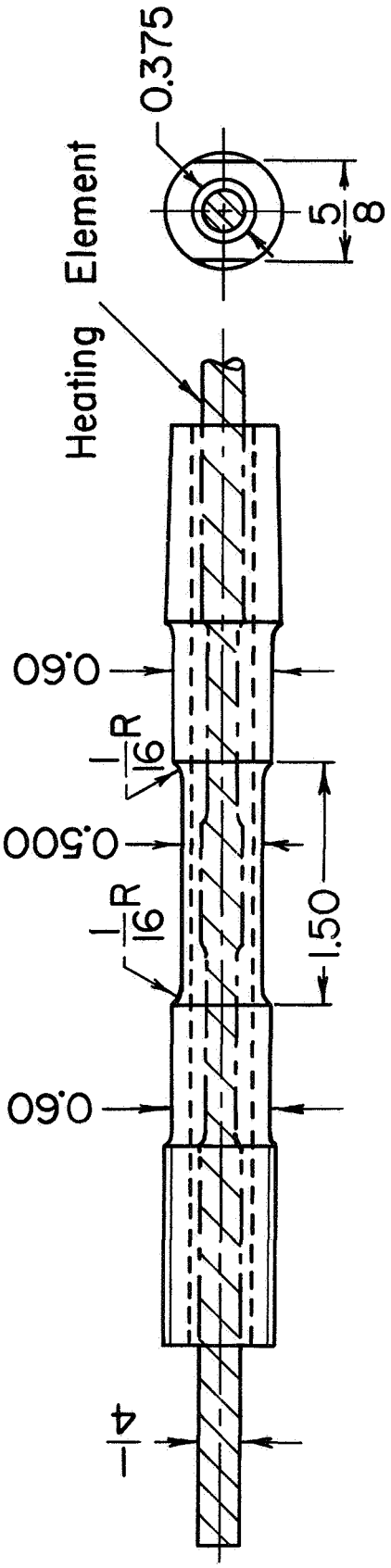

Fig.2 Specimen and Heating Element. All Dimensions in Inches

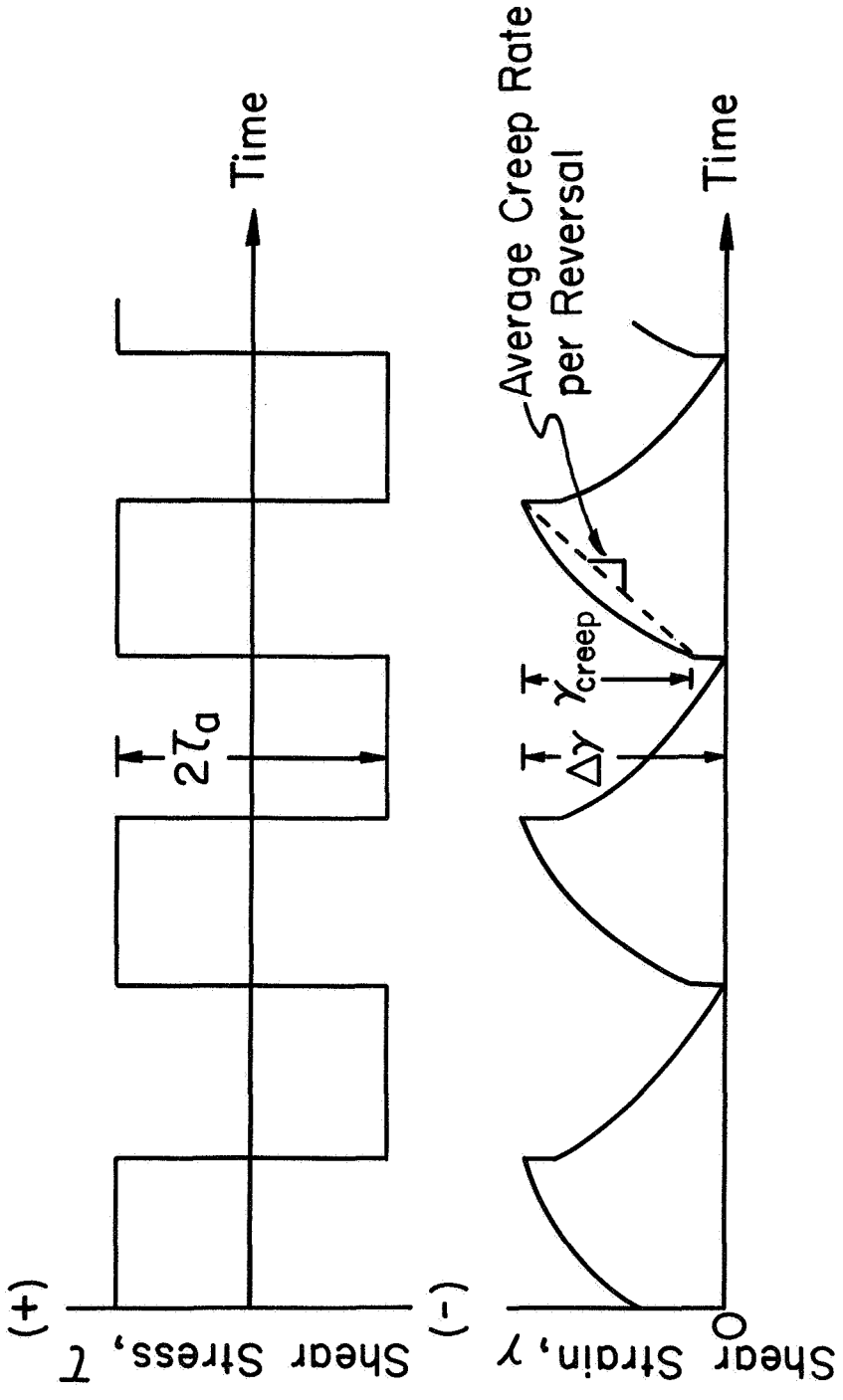

Fig. 3 Schematic Stress–Time and Strain–Time Curves

(b) Transverse Cross Section

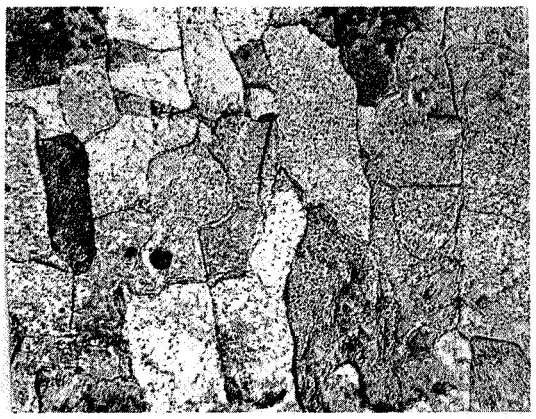

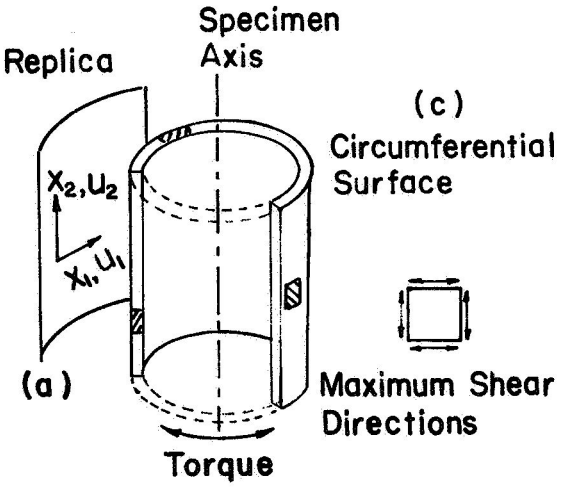

(d) Longitudinal Cross Section

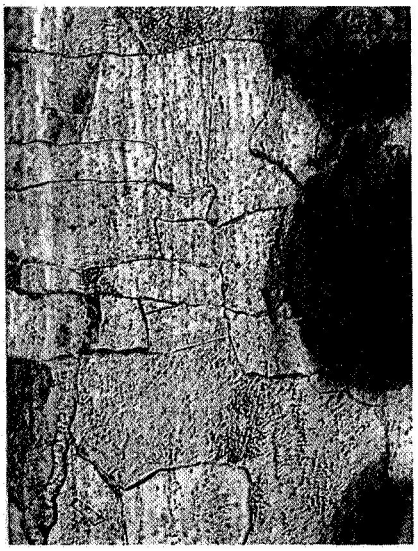

Fig. 4 Cross Sections and Surface of a Specimen after Reversed Creep ($T = 0.5T_m$, $\tau_a = \pm 640$ psi, $\Delta\gamma = 0.047$) Showing that Grain Shape Is Orthorhombic.

0.2 mm

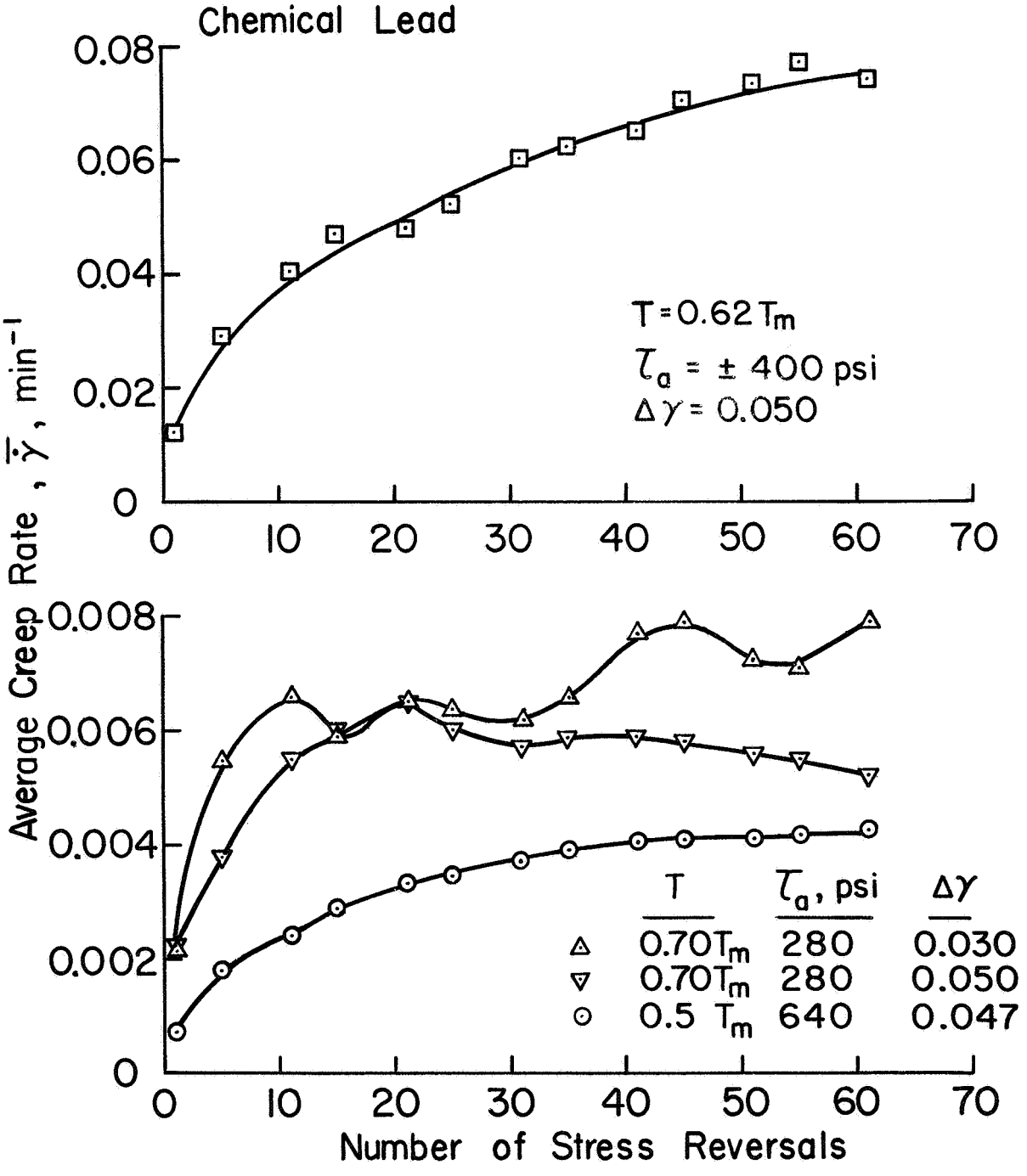

Fig. 5 The Change in Average Creep Rate during Reversed Creep

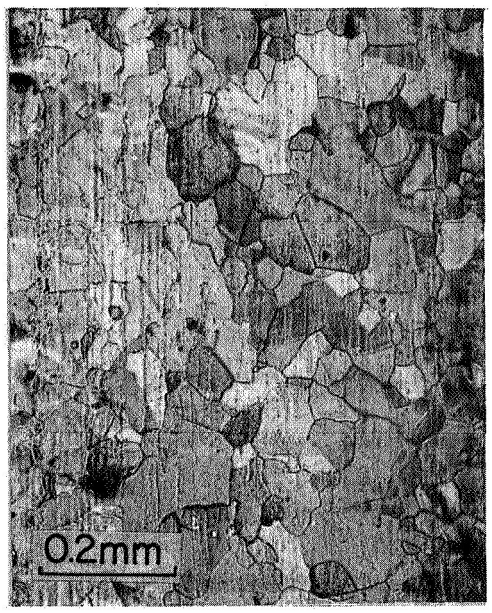

(a) Before Testing

(b) After Reversed Creep, $T=0.5\,T_m$, $\tau_a = \pm 640$ psi, $\Delta\gamma = 0.047$

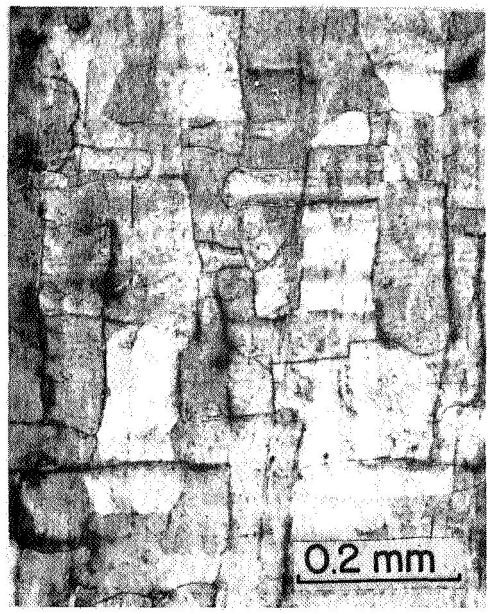

(c) After Reversed Creep, $T=0.62\,T_m$, $\tau_a = \pm 460$ psi, $\Delta\gamma = 0.050$

(d) After Reversed Creep, $T=0.70\,T_m$, $\tau_a = \pm 280$ psi, $\Delta\gamma = 0.030$

Fig. 6 Surface of Chemical Lead Specimens after Reversed Creep at Various Temperatures (After Chemical Polishing)

Max. Shear Directions

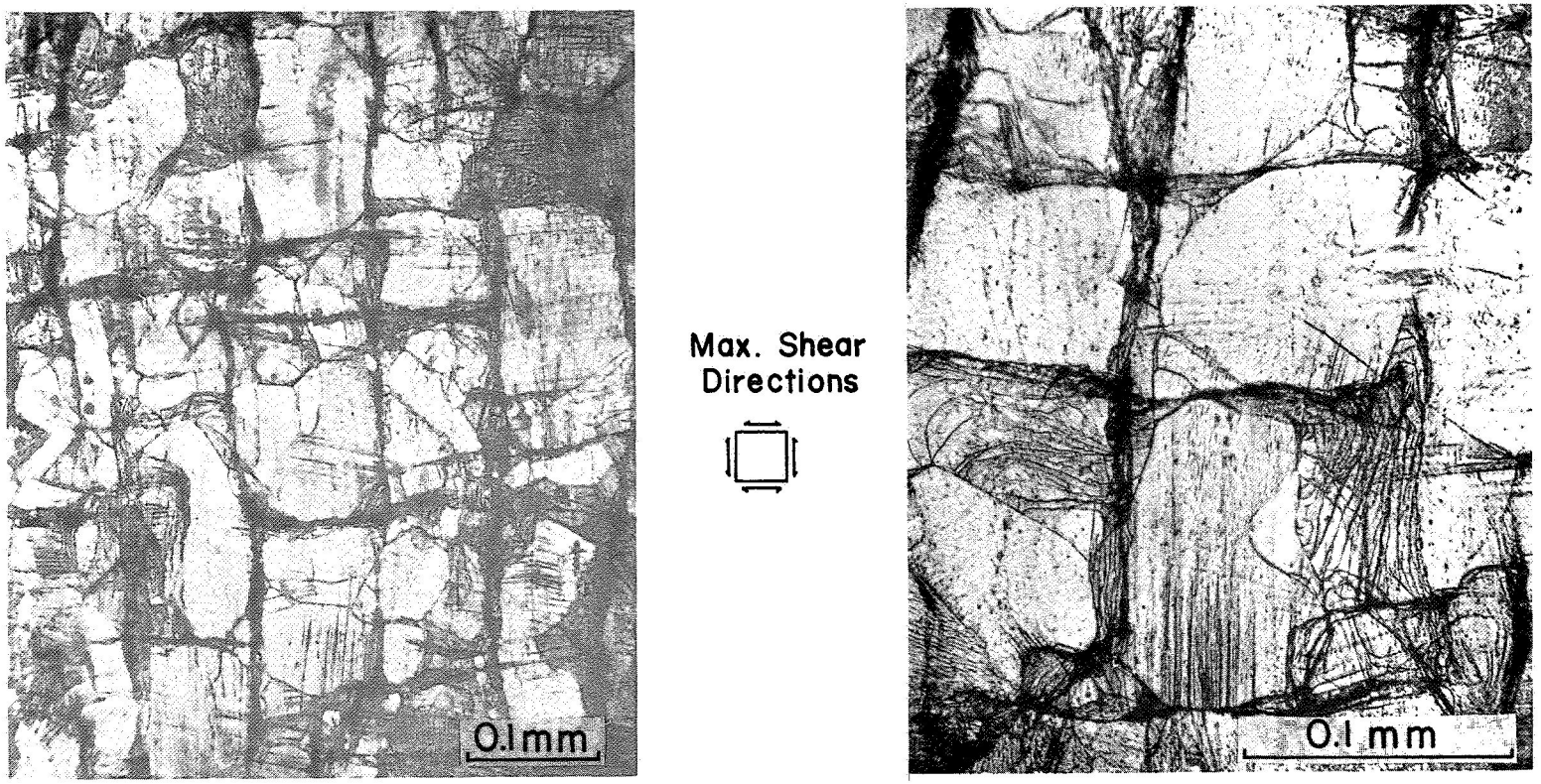

Fig.7 Surface of a Specimen after Reversed Creep under $T=0.5T_m$, $\Delta\gamma=0.047$, $\tau_a=\pm640$ psi, Showing the Trace of Grain Boundary Migration, Severely Deformed Region and Intense Slip Bands near T- and L-Type Intersections of Grain Boundaries (Before Chemical Polishing).

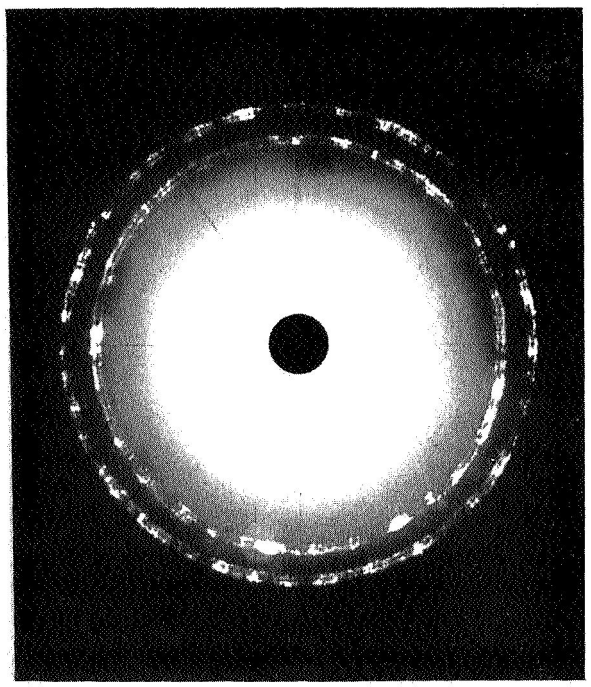

Fig.8 A Representative X-ray Diffraction Pattern of Chemical Lead after Reversed Creep under $\tau_a = \pm 640$psi, $T = 0.5T_m$, $\Delta\gamma = 0.047$ (Cu-K_α Radiation, Beam Diameter 1 mm).

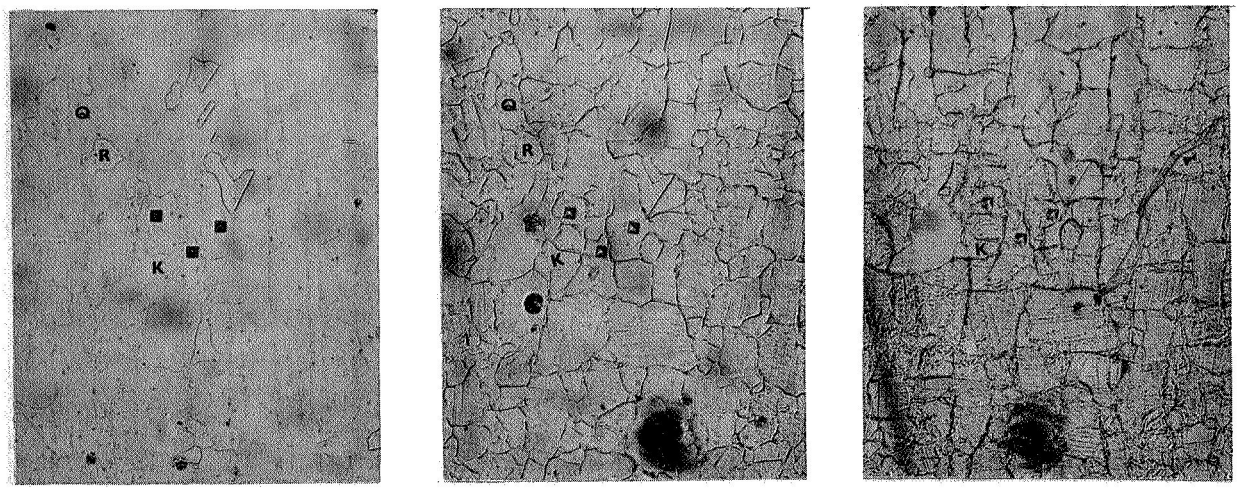

(a) Before Test (b) First Reversal (c) 15th Reversal

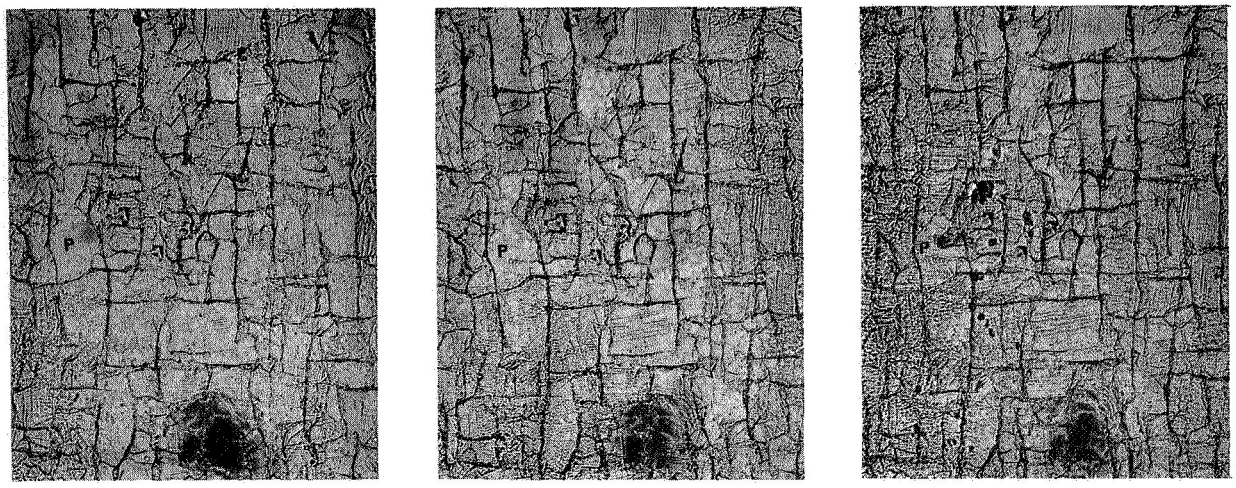

(d) 28th Reversal (e) 40th Reversal (f) 67th Reversal

0.5mm

Fig. 9 Periodic Observation of Grain Structure during Reversed Creep Test, Showing the Progressive Formation of a Rectangular Network of Grain Boundaries

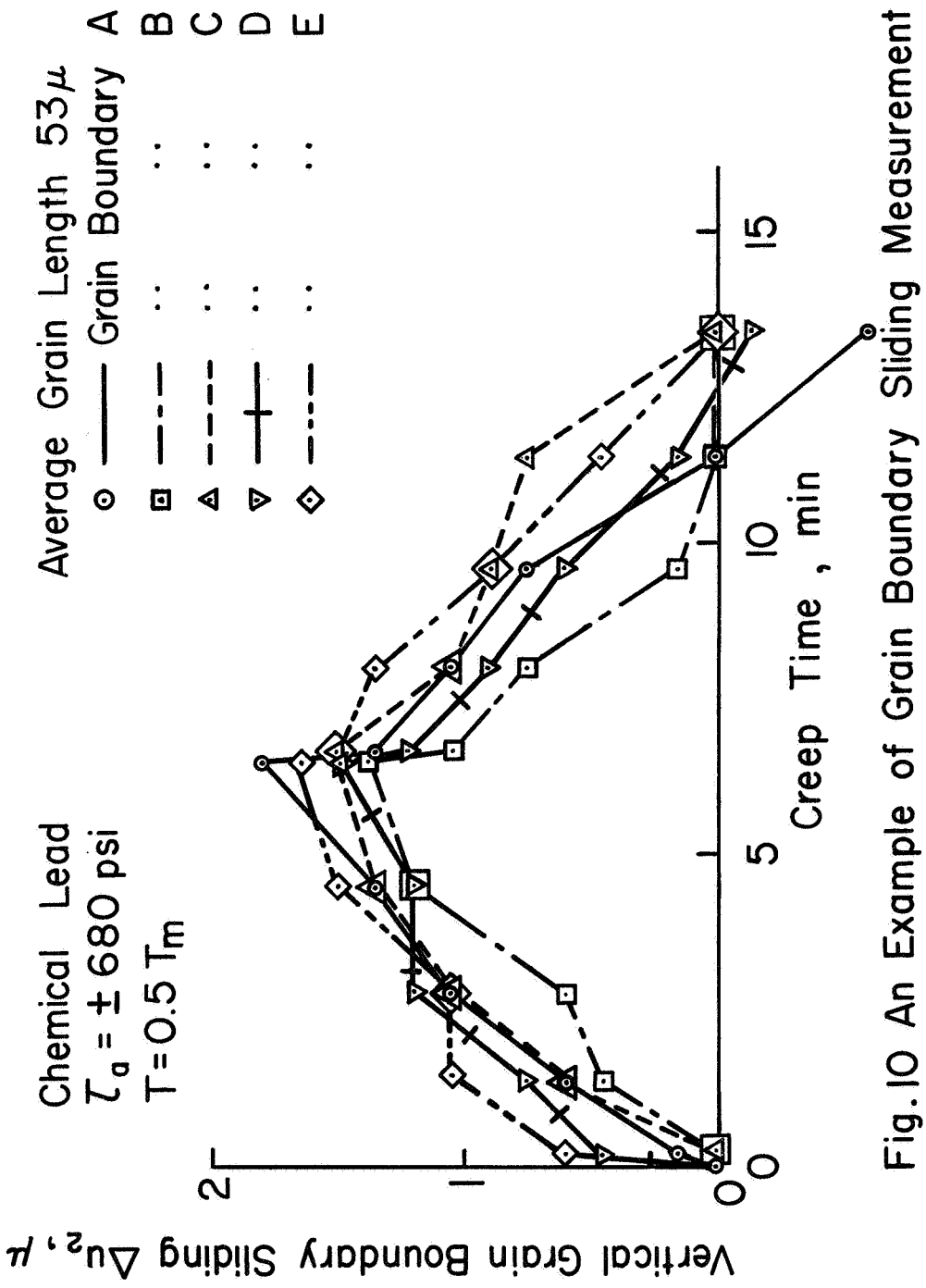

Fig. 10 An Example of Grain Boundary Sliding Measurement

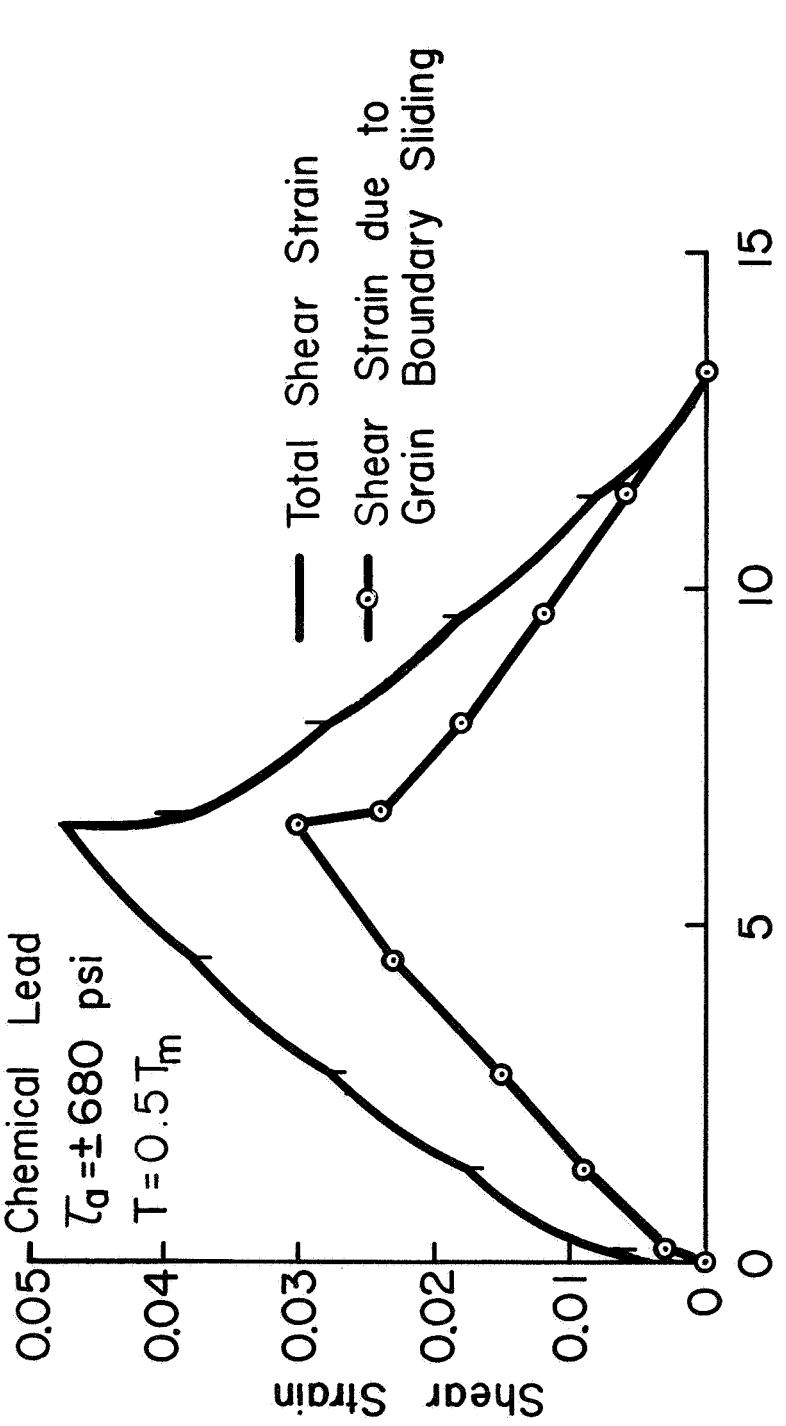

Fig. 11a Grain Boundary Sliding Strain in the Orthorhombic Grain Structure Compared with the Total Creep Strain

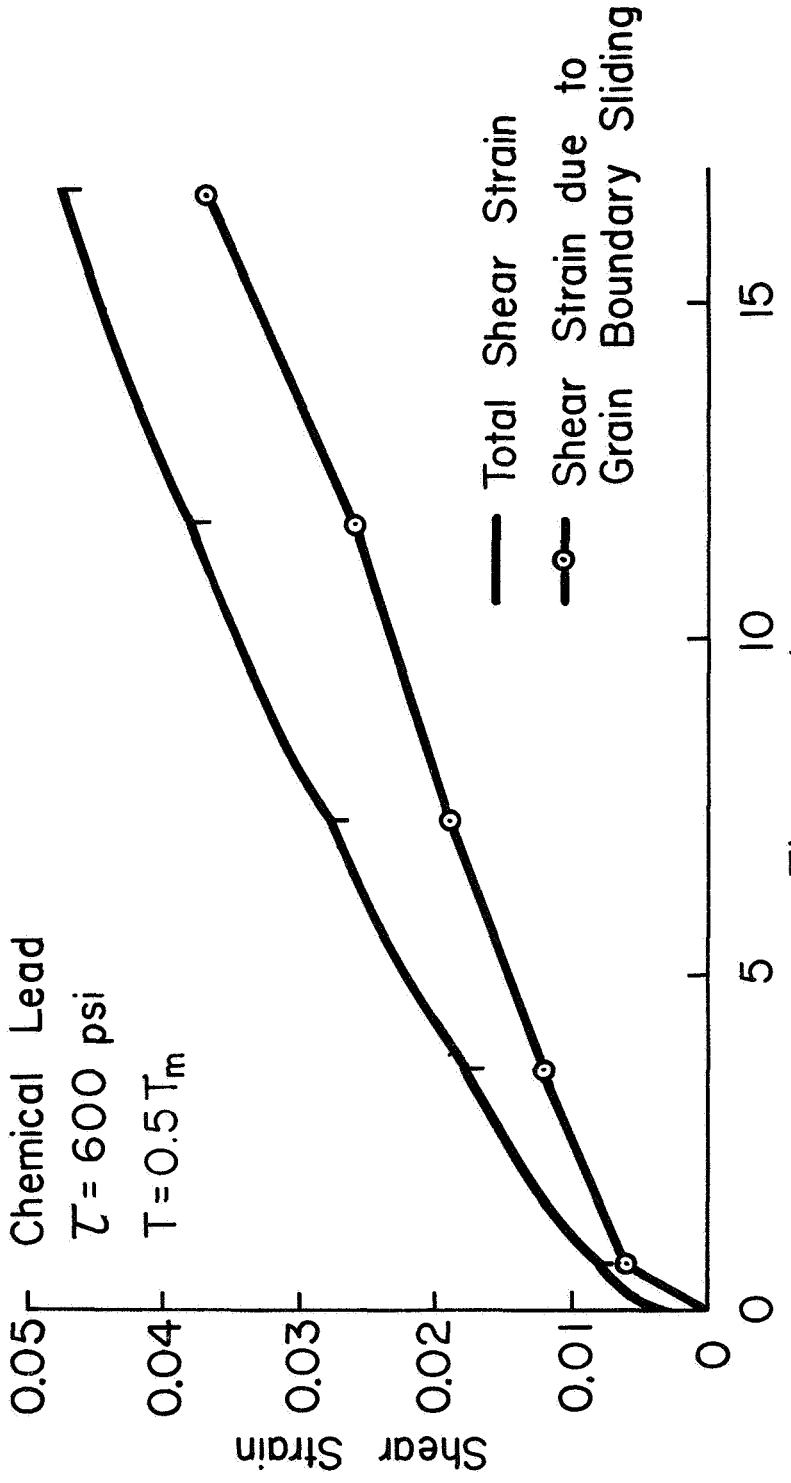

Fig. 11 b Grain Boundary Sliding Strain in the Orthorhombic Grain Structure Compared with the Total Creep Strain

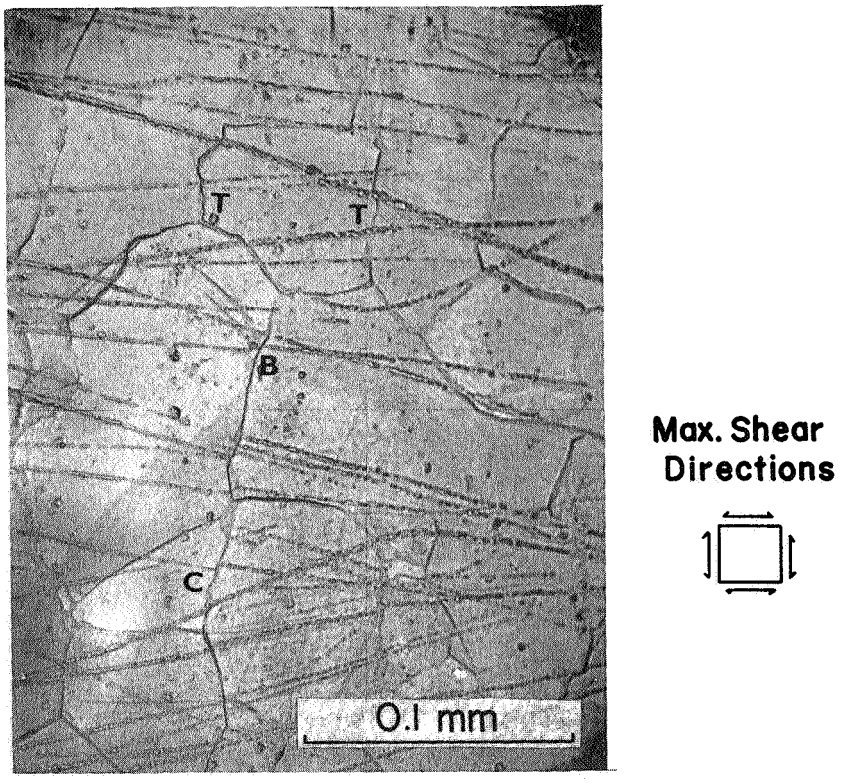

Fig. 12 Grain Boundary Sliding during Static Creep in the Irregularly Shaped Grain Structure ($T = 0.5 T_m$, $\tau = 600$ psi, $\gamma_t = 0.047$).

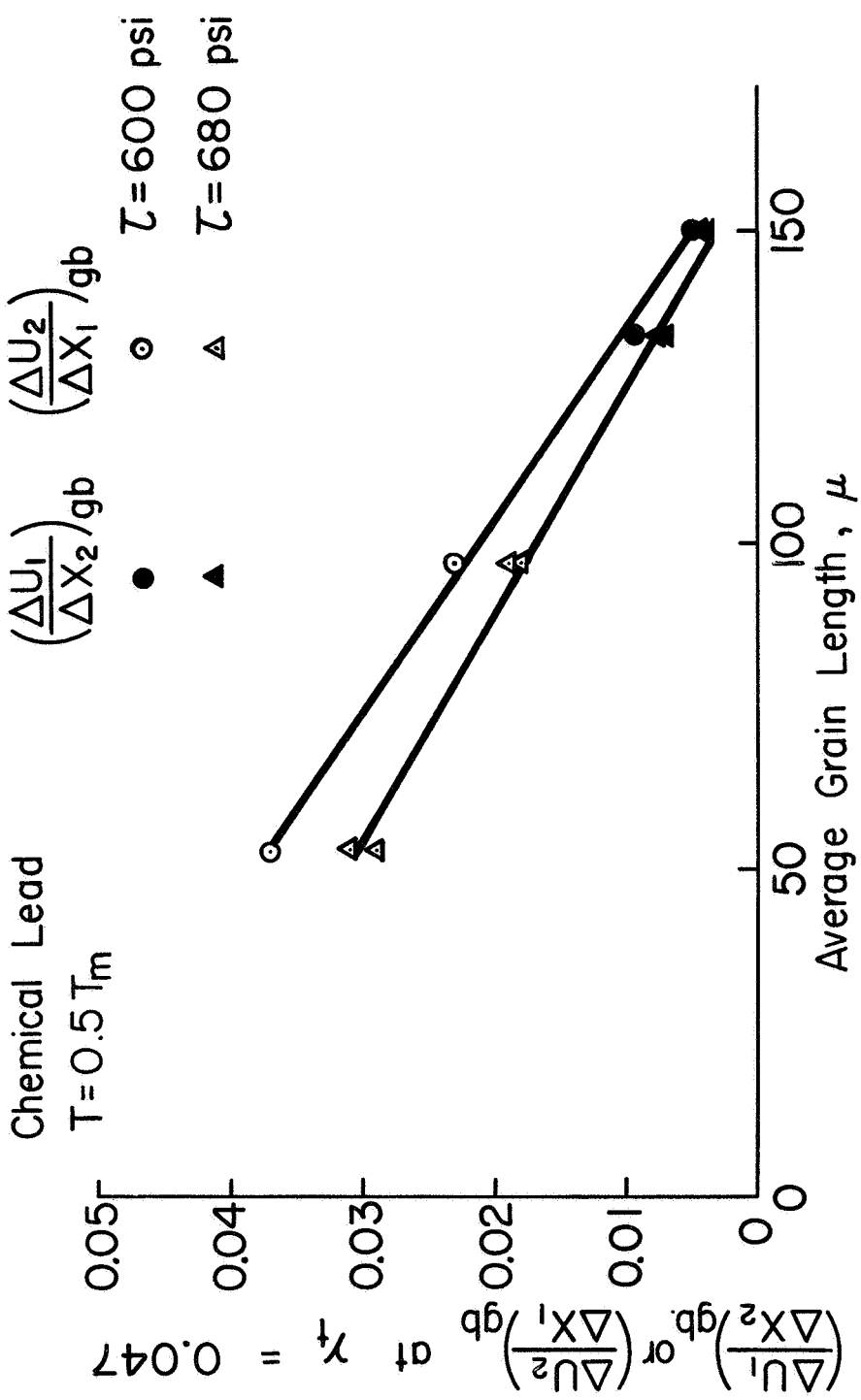

Fig. 13 Grain Boundary Sliding in the Orthorhombic Grain Structure as a Function of Grain Length

Recent T. &A. M. Reports

No.	Title	Date
297	"Blade Chanel Flow in a Simulated Radial-Flow Turbomachine," by R. C. Hansen.	June 1967
298	"Dispersion of Flexural Waves in Circular, Bi-Material Cylinders," by R. C. Reuter, Jr.	July 1967
299	"Factors Influencing the Plane Strain Crack Toughness Values of a Structural Steel," by A. K. Shoemaker.	July 1967
300	"On Terminal Crack Velocities in Brittle Materials," by M. H. Sadd.	August 1967
301	"Piecewise Polynomials and the Partition Method for Ordinary Differential Equations," by H. L. Langhaar and S. C. Chu.	September 1967
302	"A Comparison Plain Strain Fracture Toughness in the Isothermal Flow Properties of a Structural Steel," by W. Koves.	August 1967
303	"Preliminary Investigation of Measurement of Elastic Moduli of Composites Using Strain Gages," by G. Trantina.	September 1967
304	"A Sequentially Modulated Ruby Laser System for Transmitted and Scattered Light Dynamic Photoelasticity," by R. Rowlands.	September 1967
305	"Crack Control in One Way Slabs Reinforced with Deformed Welded Wire Fabric," by J. Lloyd, H. Rejali, and C. E. Kesler.	October 1967
306	"Splice Requirement for Deformed Wire Fabric in One Way Slabs," by J. Lloyd and C. E. Kesler.	December 1967
307	"Modes of Failure of Glass Fiber Reinforced Plastics Under Compressive Loads," by J. W. Gillman and H. T. Corten.	September 1967
308	"Low Cycle Fatigue Properties of an Ausformed Steel," by J. E. Matheny.	February 1968
309	"Discontinuous Mode of Crack Extension in Unidirectional Composite," by E. M. Wu and H. T. Corten.	March 1968
310	"Turbulent Friction in Eccentric Annular Conduits," by J. M. Robertson.	March 1968
311	"Alleviation of Fatigue Damage," by B. I. Sandor.	March 1968
312	"Environmental Cracking in AISI 4340 Steel," by W. A. Van Der Sluys.	April 1968
313	"The Conference on the Matrix of Concrete," by J. L. Lott.	April 1968
314	"Fracture Toughness of Portland Cement Concretes," by D. Naus and J. L. Lott.	May 1968

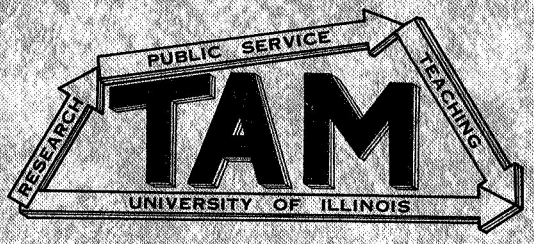
PUBLIC SERVICE
RESEARCH
TEACHING
TAM
UNIVERSITY OF ILLINOIS